



Chitosan, from crayfish wastes, as a Possible Therapeutic Option against COVID-19; an In- Silico Perspective

Salwa A.H. Hamdi¹ and Abdo A. Elfiky^{2*}

1. Zoology Department, Faculty of Sciences, Cairo University, Giza, Egypt.;

2. Biophysics Department, Faculty of Sciences, Cairo University, Giza, Egypt.;

*Corresponding Author: dr_abdo@cu.edu.eg

ARTICLE INFO

Article History:

Received: March 1, 2022

Accepted: March 12, 2022

Online: April 11, 2022

Keywords:

Chitosan,
SARS-CoV-2,
Viral attachment,
Spike protein,
Host-cell recognition,
GRP78

ABSTRACT

Human coronavirus SARS-CoV-2 is the causative agent for the COVID-19 pandemic we are encountering nowadays. With the rapid spread of the contagious virus, it is urgent to find possible therapeutics. Chitosan is a naturally occurring polymer found in animals and plants. Antiviral and antibacterial activities of chitosan were documented. In the current study, the association of chitosan with the viral spike protein was assessed utilizing computational techniques. Molecular docking, combined with molecular dynamics, was used to test the binding affinity of chitosan to SARS-CoV-2 spike protein. The results suggest excellent binding potency of the chitosan to SARS-CoV-2 spike receptor-binding domain (RBD). These results are based on the docking and the interaction dynamics. Chitosan was able to form eight contacts (H-bonds and few salt bridges) with the spike receptor-binding domain (RBD) near the angiotensin-converting enzyme 2 (ACE2) and glucose regulating protein 78 (GRP78) recognition surfaces. Thus, chitosan can be a successful candidate against COVID-19; however, the in-silico results are yet to be validated experimentally. The current data were submitted to the Egyptian Academy of Scientific Research and Technology (ASRT) patent office with the registration number of 1602/2020.

INTRODUCTION

COVID-19 pandemic causes a lot of socio- economic burden worldwide (Ali & Alharbi, 2020). The novel human coronavirus (HCoV) strain SARS-CoV-2 (severe acute respiratory syndrome coronavirus-2) is the causative agent for the COVID-19 pandemic. SARS-CoV-2 belongs to the beta coronavirus family of the human coronaviruses and was first identified two years ago in China (Elfiky, 2020). Different proteins compose the viral particle, including spike (S), envelope (E), nucleocapsid (N) and membrane (M) proteins (Elfiky *et al.*, 2017). Due to the importance of understanding the mode of internalization of the virus particles, the spike protein sheds researchers as a crucial protein target (Elfiky, 2020; Adem *et al.*, 2021). The first structure (solved

experimentally) for the spike protein was released in the protein data bank in February 2020 (PDB ID: 6VSB) (Wrapp *et al.*, 2020).

Different host cell receptors were reported to facilitate the viral entry, including the angiotensin-converting enzyme 2 (ACE2) and the glucose regulating protein 78 (GRP78) (Elfiky, 2020; Ha *et al.*, 2020; Ibrahim *et al.*, 2020; Saghazadeh & Rezaei, 2020; South *et al.*, 2020). The Receptor Binding Domain (RBD) found in the S1 region of the spike is the recognition site for host cell receptors.

Chitosan is a linear polymer of a (β 1-4)-linked 2-amino-2-deoxy-b-D-glucopyranose derived by N-deacetylation of chitin. It is a hetero-polymer of a fiber-like substance consisting of N-acetyl glucosamine and D-glucosamine units distributed among the chain. Chitin comes after cellulose as the second most abundant organic compound. The shellfish waste of crustaceans such as crawfish, shrimps, and crabs are considered the primary sources of chitosan (Kim 2018).

Chitosan is a highly basic polysaccharide, linear polyamine, with reactive amino groups, reactive hydroxyl groups, and it chelates many transitional metal ions. Chitosan as a biopolymer has some biological properties. It shows biocompatibility and biodegradability based on the degree of deacetylation and molecular weight (Fei Liu *et al.*, 2001; Mady *et al.*, 2009; Mady & Darwish, 2010). Other essential characteristics of chitosan are viscosity and solubility. Viscosity is important in determining chitosan's molecular weight, as higher chitosan molecular weight often renders a higher viscous solution, which is difficult in handling. Chitosan is characterized by its higher solubility in dilute organic acids, such as acetic acid, formic acid, and lactic acid, compared to inorganic acids. Additionally, the solubility of chitosan is poor in solvents with pH 7.00. Its biocompatibility, biodegradability, and non-toxicity enable chitosan to be used in biomedical, industrial, environmental and biotechnological investigations (Hamdi, 2019). Chitosan has numerous biological activities, including antimicrobial activities, antioxidant properties, immune-enhancing effects and antitumor activity (Zhang *et al.*, 2010). Chitosan's biomedical applications include drug delivery, wound dressings, implant coatings, tissue engineering, and therapeutic agent delivery systems (Wilson *et al.*, 2011).

Computational methods have become a routine work nowadays in drug designs (Ganesan & Barakat, 2017; Abu-Melha *et al.*, 2020; Elfiky, 2020a, 2020b; Elfiky *et al.*, 2020, Elfiky & Ibrahim, 2021; Mahmud *et al.*, 2021). They can predict the atomic and molecular properties of the 3D structures (Leach 2001, Sonousi *et al.* 2021). In this study, chitosan's binding affinity to the SARS-CoV-2 spike protein is tested using computational methods. Molecular docking combined with dynamics simulation can prove the binding affinity of the chitosan to the receptor-binding domain of the SARS-CoV-2, where host-cell recognition occurs.

MATERIALS AND METHODS

The spike protein's 3D structure for SARS-CoV-2 was downloaded from the Protein Data Bank (PDB ID: 6YLA, chain A) <https://www.rcsb.org/>. There is no 3D structure for chitosan, so the 2D structure is downloaded from the PubChem database (CID: 71853) <https://pubchem.ncbi.nlm.nih.gov/>. After that, the 3D model for chitosan was built using Avogadro software (**Hanwell et al. 2012**). Energy minimization is performed using the Universal Force Field (UFF) and the steepest descent algorithm (**Fliege and Svaiter 2000**). After minimization, any missed Hydrogen atoms and charges are added using AutoDock Tools software (**Morris et al. 2009**). Additionally, the structure of the SARS-CoV-2 spike also is prepared for docking using AutoDock Tools.

Molecular Dynamics Simulation

The SARS-CoV-2 spike structure (PDB ID: 6YLA) is subjected to 100 ns MDS using Nanoscale Molecular Dynamics (NAMD) 2.13 software (**Phillips et al. 2005**). CHARMM 36 force field is utilized, while the TIP3P water model is used at 310 K. The protein/water system is ionized using NaCl for the solution to be with a salt concentration of 0.154 M at pH 7 using the visualizing Molecular Dynamics (VMD) 1.9.3 software (**Humphrey et al. 1996**). VMD is also used in analyzing the MDS data after the 100 ns run. The equilibration and the production runs are performed on the Bibliotheca Alexandrina high-performance computing facility, Alexandria, Egypt (24 parallel cores). Cluster analysis is performed after the production run using UCSF Chimera software (**Pettersen et al. 2004**). A representative structure from each cluster is used in the docking study.

Docking experiments

The prepared structures (SARS-CoV-2 spike after MDS and the chitosan 3D model) are utilized with the AutoDock Vina software (**Trott and Olson 2010**). The docking protocol uses the spike receptor-binding domain (RBD) as the target for docking. The docking was performed on an HP Z400 workstation utilizing eight-core parallel runs. The box sizes were about $126 \times 126 \times 126 \text{ \AA}^3$, while centered at about $(-12, -7, -16) \text{ \AA}$. Protein-ligand interaction profiler (PLIP) web server (<https://plip-tool.biotec.tu-dresden.de/plip-web/plip/index>) is used to check the docking complexes for established interactions upon docking (**Salentin et al. 2015**).

RESULTS

1. Molecular dynamics simulation

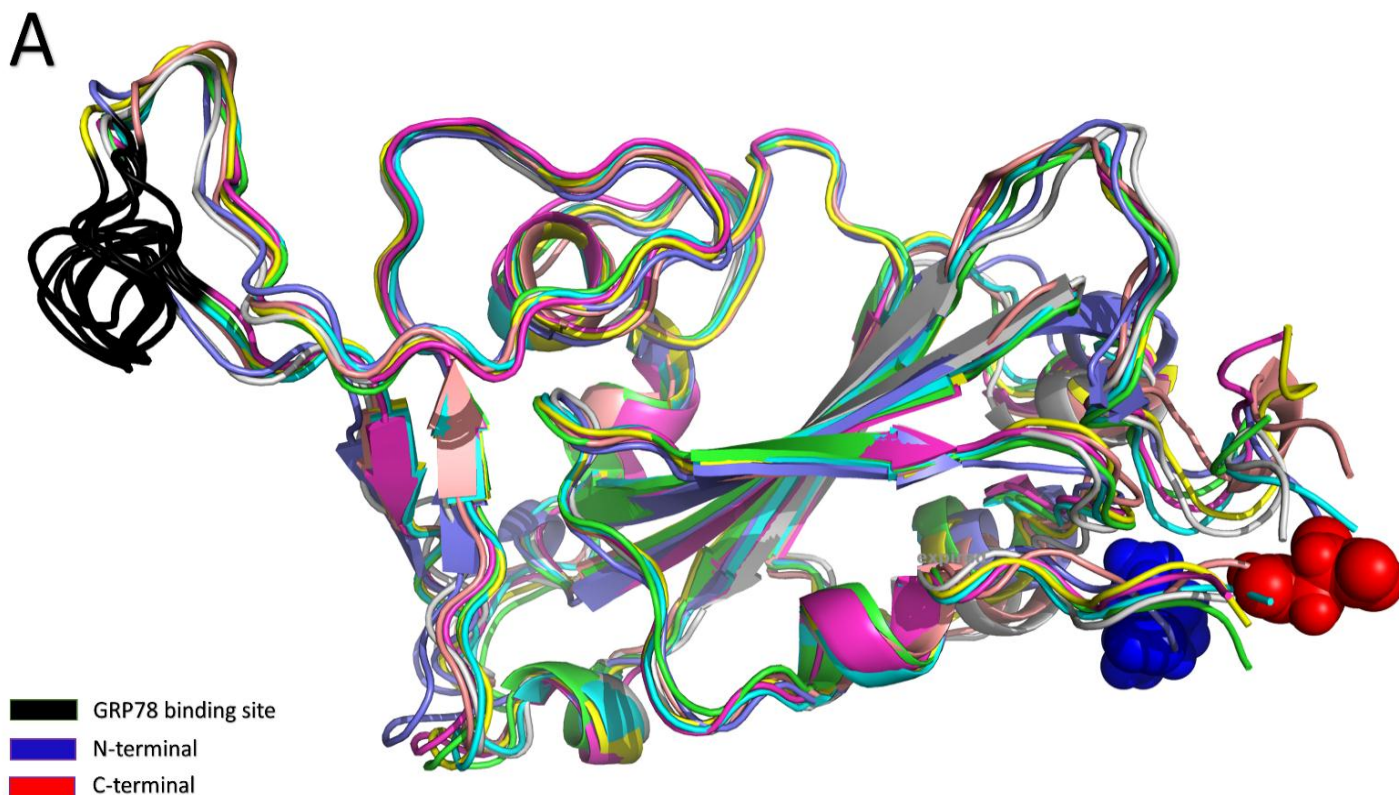
Figure 1A shows the superposition of the spike protein's seven different conformations (PDB ID: 6YLA) after performing the MDS run for 100 ns. Each conformation represents a cluster of trajectories. The conformations are taken at 4.9 ns, 13.3 ns, 22.5 ns, 33.7 ns, 44.5 ns, 71.7 ns, and 88.1 ns. Each conformation is represented

by a colored cartoon, while the GRP78-binding site (C480-C488) that we predict in a previous study (Ibrahim *et al.* 2020) is shown in the black cartoon. The N-terminal and the C-terminal residues are shown in blue balls and red balls, respectively. Figure 1B shows the per-residue root mean square fluctuations (RMSF) in Å.

2. Molecular docking

Figure 2 shows chitosan's binding energies (in kcal/mol) against the seven different conformations of the SARS-CoV-2 spike RBD gotten after MDS. Additionally, Table 1 summarizes the interaction pattern observed for the docking experiments.

Figure 3A shows the superposition of the docking complex of chitosan (red sticks) with RBD of SARS-CoV-2 spike (cyan cartoon) at 44.5 ns conformation and the solved structure (PDB ID: 6ACK) of SARS-CoV-2 spike (green cartoon) bound to ACE2 (magenta cartoon).



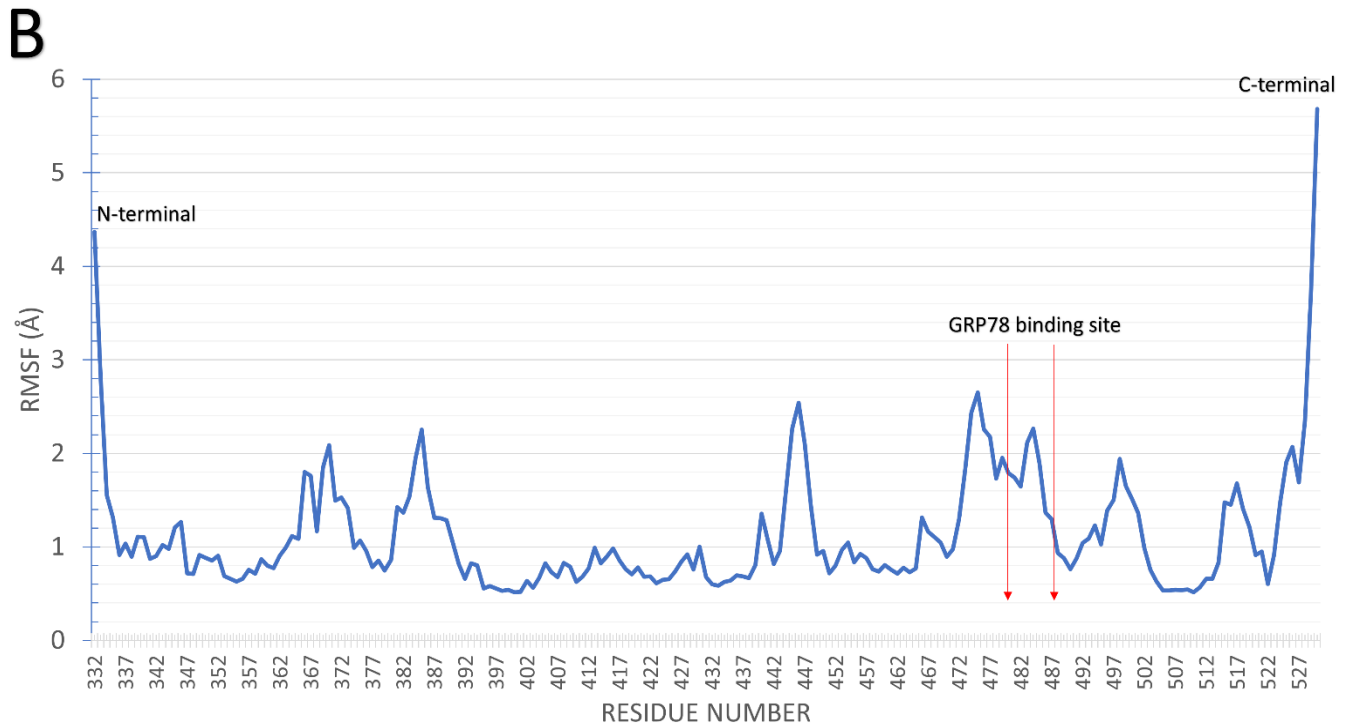


Figure 1 SARS-CoV-2 spike receptor-binding domain dynamics. (A) The superposition of the different conformations of the spike RBD after 100 ns MDS. Each conformation represents a cluster of trajectories. N and C- termini of the RBD are depicted in blue and red balls, respectively, while the GRP78 recognition site is in black ribbons. (B) The RMSF in Å versus residue numbers during the 100 ns MDS run.

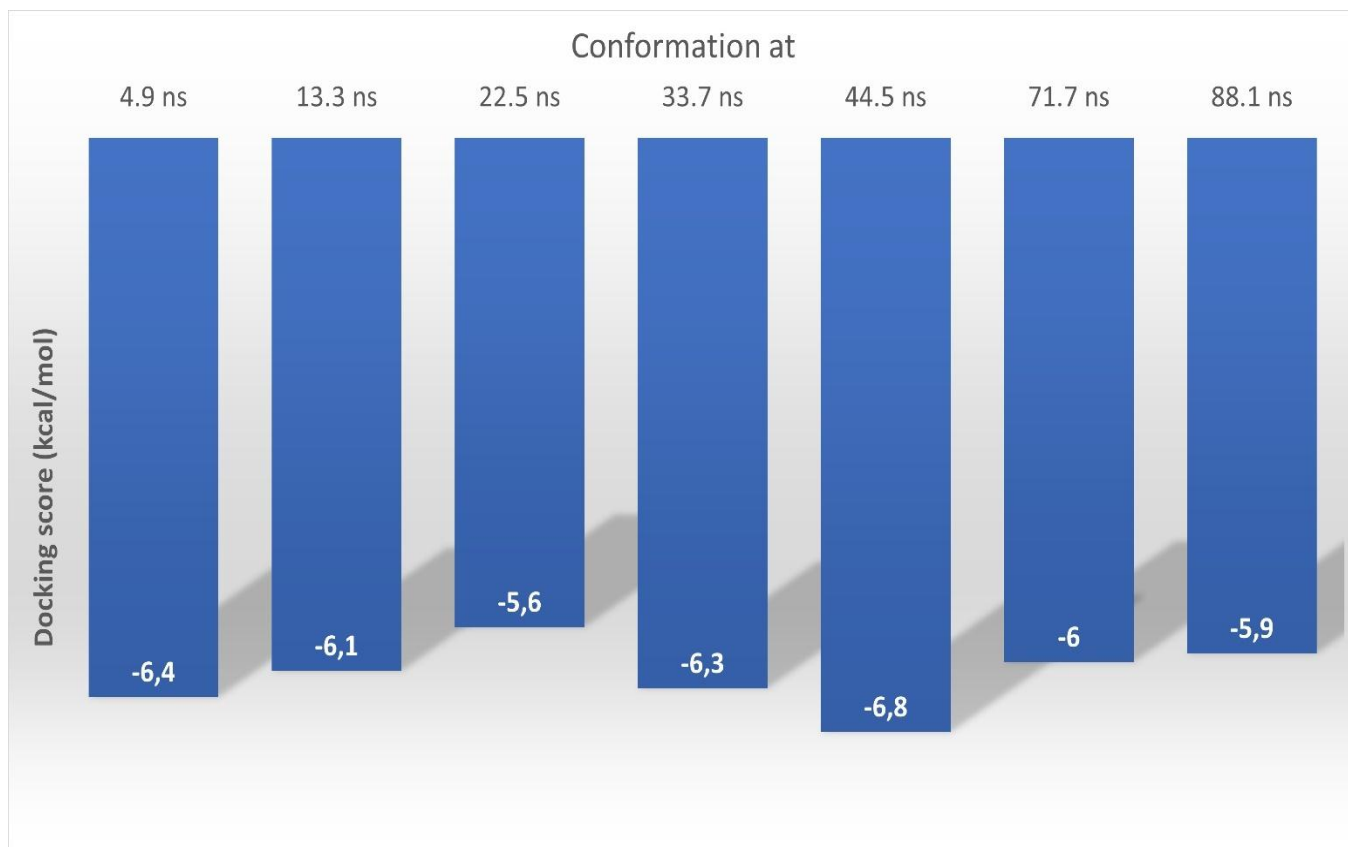


Figure 2 The binding affinities in kcal/mol for the different conformations of the SARS-CoV-2 Spike RBD to Chitosan calculated using AutoDock Vina software.

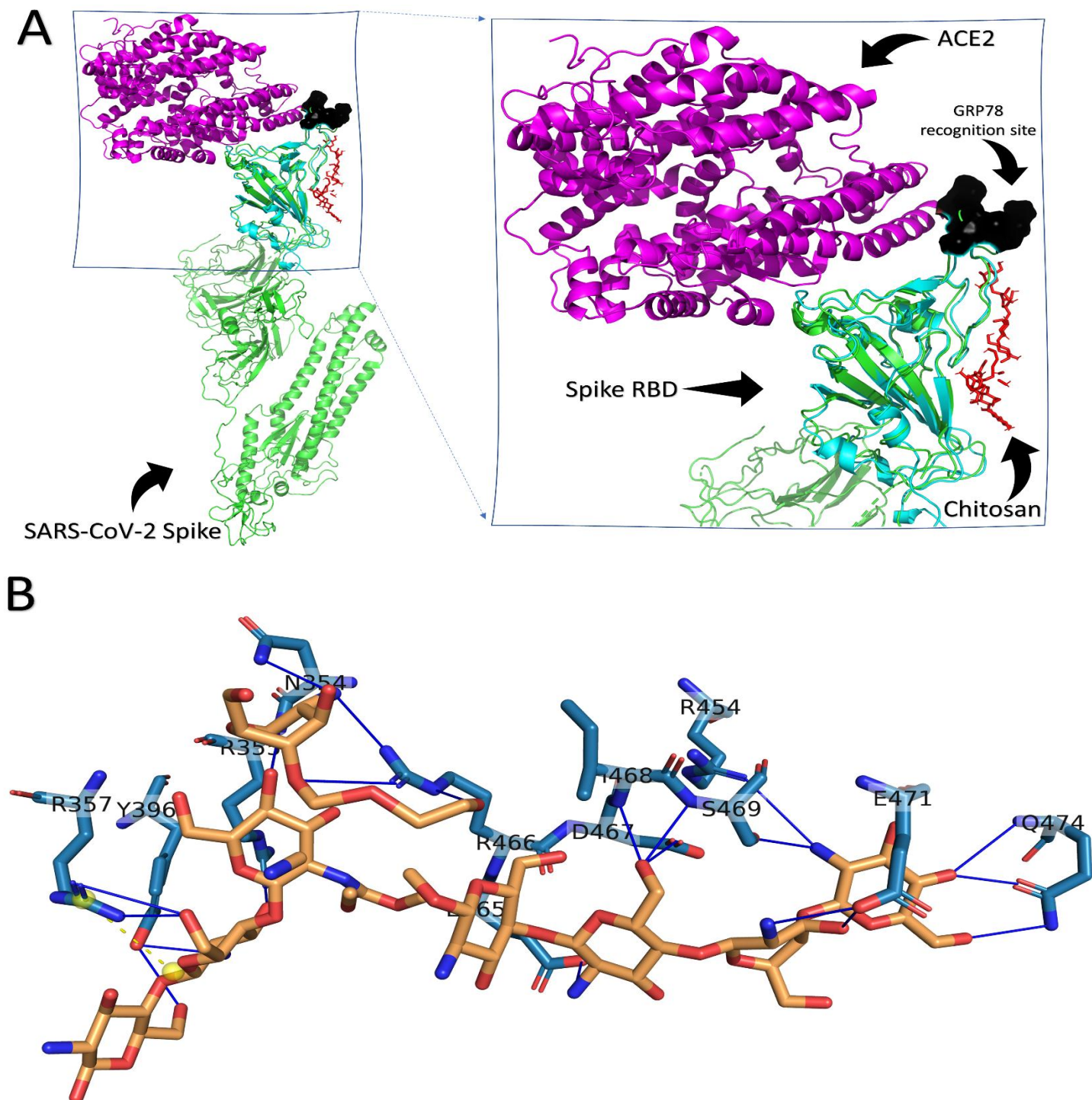


Figure 3 (A) The superposition of the solved structure for SARS-CoV-2 Spike (PDB ID: 6ACK) protein (green cartoon) bound to ACE2 (magenta cartoon) and the docking complex of the RBD of SARS-CoV-2 Spike (PDB ID: 6YLA) protein (cyan cartoon) docked with Chitosan (red sticks). The black surface represents the GRP78 binding site on SARS-CoV-2 Spike (C480-C488). (B) An enlarged panel showing the formed interactions between Chitosan (yellow) and RBD of SARS-CoV-2 spike residues (cyan).

Table 1 The detailed interactions reported for Chitosan to SARS-CoV-2 spike RBD different conformation after the MDS.

<i>Conformation of SARS-CoV-2 Spike at</i>	<i>AutoDock Vina score (kcal/mol)</i>	<i>H-bonding</i>		<i>Salt bridges</i>	
		number	Residues from SARS-CoV-2 spike RBD Take part in the interaction	number	Residues from SARS-CoV-2 spike RBD Take part in the interaction
4.9 ns	-6.4	15	R355(2), R357(3), R454, E465(2), D467, I468, S469, E471(2), I472, and S514	2	R457(2)
13.3 ns	-6.1	12	I332, N334, S383, C391, L517, A520(3), A522, C525, K529, and T531	0	
22.5 ns	-5.6	19	T345(3), R346(6), A348, S349(3), N354, K356, S399, N448, Y449, and N450	1	K356
33.7 ns	-6.3	12	R355, R357(2), K458, E465, R466(3), D467, S469, E471, and I472	2	R457(2)
44.5 ns	-6.8	23	N354, R355(2), R357(2), Y396(3), R454, E465, R466(3), D467, I468, S469(2), E471(3), and Q474(3)	1	R357
71.7 ns	-6.0	16	Y369(2), N370, A372, F374, S375(4), T376, F377(2), K378, Y380, and Y508(2)	1	K378
88.1 ns	-5.9	18	Y369, S375, T376(4), F377(3), K378, C379, Y380, G404(2), D405, V407, and R408(2)	1	K378

DISCUSSION

The SARS-CoV-2 spike-host cell recognition is crucial in fighting the COVID-19 both as a therapeutic and prophylactic route. It was reported that various natural compounds could stop viral infections or improve the patients' immune system (**Adem *et al.* 2020, Elfiky *et al.* 2020, Elfiky 2021**). Chitosan is found in various sources, including marine animals and different plants (**Zhang *et al.* 2010**).

Figures 1 A and 1B reflect that the most flexible residues are the terminal residues with RMSF values ≥ 4 Å. The other residues, including the GRP78-binding site region (C480-C488), experience RMSF values less than 2.7 Å. Therefore, this region could be considered stable during the 100 ns simulation period.

As reflected from the binding energies (Figure 2), chitosan has an excellent binding affinity against SARS-CoV-2 spike RBD ranging from -5.6 kcal/mol down to -6.8 kcal/mol. Now we need to check how the binding was established by checking the docking poses.

H-bonds are the primary interactions established upon docking with few salt bridges reported in some conformations of the SARS-CoV-2 spike RBD. At least 12 H-bonds stabilize the binding with one or two salt bridges reported in Table 1 (13.3 ns conformation is an exception with missing salt bridges). The bold residues in Table 1 represent the ACE2 binding surface of the SARS-CoV-2 spike RBD. This means that chitosan binding to RBD may interfere with recognizing the SARS-CoV-2 spike by the primary host cell receptor, as shown with more than half (4 out of 7) the conformations we used in the docking study.

As shown in the figure, the chitosan is attached near the ACE2 binding surface. Additionally, as shown in Figure 3B, 21 H-bonds (blue lines) are formed between chitosan and 12 residues of SARS-CoV-2 spike RBD. These residues are R353, N354, R357, Y396, R454, L465, R466, D467, I468, S469, E471, and Q474, while R357 forms a salt bridge as well to chitosan (dashed-yellow line). These residues lie near the ACE2 binding surface (K417, G446, Y449, N487, Y489, Q493, T500, N501, G502, and Y505), and the GRP78 recognition region (C480-C488) of the SARS-CoV-2 spike RBD (**Lan *et al.* 2020, Elfiky *et al.* 2021, Ibrahim *et al.* 2021**). This suggests chitosan's possibility of contradicting SARS-CoV-2 spike recognition through host-cell receptors (ACE2 and GRP78).

Conclusively, chitosan can bind to SARS-CoV-2 spike RBD with an excellent binding affinity (-6.16 ± 0.36 kcal/mol). Furthermore, chitosan's binding is stabilized by more than 12 H-bonds and few salt bridges to the ACE2 recognition site. Thus, the chitosan binding may interfere with host cell recognition of SARS-CoV-2. The vast availability of chitosan in marine animals and plants makes it superior to other medicines worth further investigation against COVID-19. Experimental validation of the results is recommended as future work.

CONCLUSION

Natural compounds prove themselves as potential therapeutic options against infectious diseases and cancer. Here we suggest the chitosan found in marine animals and plants as a possible anti-COVID-19 agent. Based on our *in silico* predictions, chitosan can bind to the spike protein at the RBD, forming H-bonds and salt bridges. Moreover, chitosan binds with the same surface that recognizes the host-cell receptors (ACE2 and GRP78), possibly affecting the viral recognition and entry to the host cell. Thus, chitosan is worth experimental testing against COVID-19 and other coronaviruses that use its spikes to enter their hosts.

Acknowledgments

Dr. Bahaa M Abdelazim and Ibrahim M Ibrahim are appreciated for their help with the computations.

REFERENCES

- Abu-Melha, S.; Edrees, M. M.; Riyadh, S. M.; Abdelaziz, M. R.; Elfiky, A. A. and Gomha, S. M. (2020). Clean Grinding Technique: A Facile Synthesis and In Silico Antiviral Activity of Hydrazones, Pyrazoles, and Pyrazines Bearing Thiazole Moiety against SARS-CoV-2 Main Protease (M(pro)). *Molecules*, 25(19): 4565. doi:10.3390/molecules25194565
- Adem, S.; Eyupoglu, V.; Sarfraz, I.; Rasul, A.; Zahoor, A. F.; Ali, M.; Abdalla, M.; Ibrahim, I. M. and Elfiky, A. A. (2021). Caffeic acid derivatives (CAFDs) as inhibitors of SARS-CoV-2: CAFDs-based functional foods as a potential alternative approach to combat COVID-19. *Phytomedicine*, 85: 153310. doi:10.1016/j.phymed.2020.153310
- Ali, I., and Alharbi, O. M. L. (2020). COVID-19: Disease, management, treatment, and social impact. *Sci Total Environ*, 728: 138861. doi:10.1016/j.scitotenv.2020.138861
- Elfiky, A. A. (2020a). Novel guanosine derivatives against Zika virus polymerase in silico. *J Med Virol*, 92(1): 11-16. doi:10.1002/jmv.25573
- Elfiky, A. A. (2020b). Reply to a letter to the editor. *Life Sci*, 252: 117715. doi:10.1016/j.lfs.2020.117715
- Elfiky, A. A. (2020c). SARS-CoV-2 Spike-Heat Shock Protein A5 (GRP78) Recognition may be Related to the Immersed Human Coronaviruses. *Front Pharmacol*, 11(1997): 577467. doi:10.3389/fphar.2020.577467

Elfiky, A. A. (2021). Natural products may interfere with SARS-CoV-2 attachment to the host cell. *J Biomol Struct Dyn*, 39(9): 3194-3203. doi:10.1080/07391102.2020.1761881

Elfiky, A. A.; Baghdady, A. M.; Ali, S. A. and Ahmed, M. I. (2020). GRP78 targeting: Hitting two birds with a stone. *Life Sci*, 260: 118317. doi:10.1016/j.lfs.2020.118317

Elfiky, A. A., and Ibrahim, I. M. (2021). Zika virus envelope - heat shock protein A5 (GRP78) binding site prediction. *J Biomol Struct Dyn*, 39(14): 5248-5260. doi:10.1080/07391102.2020.1784794

Elfiky, A. A.; Ibrahim, I. M.; Amin, F. G.; Ismail, A. M. and Elshemey, W. M. (2021). COVID-19 and Cell Stress. In N. Rezaei (Ed.), *Coronavirus Disease - COVID-19* (pp.: 169-178). Cham: Springer International Publishing.

Elfiky, A. A.; Ismail, A. M. and Elshemey, W. M. (2020). Recognition of gluconeogenic enzymes; Icl1, Fbp1, and Mdh2 by Gid4 ligase: A molecular docking study. *J Mol Recognit*, 33(5): e2831. doi:10.1002/jmr.2831

Elfiky, A. A.; Mahdy, S. M. and Elshemey, W. M. (2017). Quantitative structure-activity relationship and molecular docking revealed a potency of anti-hepatitis C virus drugs against human corona viruses. *J Med Virol*, 89(6): 1040-1047. doi:10.1002/jmv.24736

Fei Liu, X.; Lin Guan, Y.; Zhi Yang, D.; Li, Z. and De Yao, K. (2001). Antibacterial action of chitosan and carboxymethylated chitosan. *Journal of applied polymer science*, 79(7): 1324-1335.

Fliege, J. and Svaiter, B. F. (2000). Steepest descent methods for multicriteria optimization. *Mathematical Methods of Operations Research*, 51(3): 479-494.

Ganesan, A. and Barakat, K. (2017). Applications of computer-aided approaches in the development of hepatitis C antiviral agents. *Expert Opin Drug Discov*, 12(4): 407-425. doi:10.1080/17460441.2017.1291628

Ha, D. P.; Van Krieken, R.; Carlos, A. J. and Lee, A. S. (2020). The stress-inducible molecular chaperone GRP78 as potential therapeutic target for coronavirus infection. *J Infect*, 81(3): 452-482. doi:10.1016/j.jinf.2020.06.017

Hamdi, S. A. H. (2019). Extraction & characterization of Chitosan from Nile water crawfish *Procambarus clarkii*, Egypt. *Ciencia e Tecnica Vitivinicola* 34(12): 1-17.

Hanwell, M. D.; Curtis, D. E.; Lonie, D. C.; Vandermeersch, T.; Zurek, E. and Hutchison, G. R. (2012). Avogadro: an advanced semantic chemical editor, visualization, and analysis platform. *J Cheminform*, 4(1): 17. doi:10.1186/1758-2946-4-17

Humphrey, W.; Dalke, A. and Schulten, K. (1996). VMD: visual molecular dynamics. *J Mol Graph*, 14(1): 33-38, 27-38. doi:10.1016/0263-7855(96)00018-5

Ibrahim, I. M.; Abdelmalek, D. H.; Elshahat, M. E. and Elfiky, A. A. (2020). COVID-19 spike-host cell receptor GRP78 binding site prediction. *J Infect*, 80(5): 554-562. doi:10.1016/j.jinf.2020.02.026

Ibrahim, I. M.; Elfiky, A. A. and Elgohary, A. M. (2021). Recognition through GRP78 is enhanced in the UK, South African, and Brazilian variants of SARS-CoV-2; An in silico perspective. *Biochem Biophys Res Commun*, 562: 89-93. doi:10.1016/j.bbrc.2021.05.058

Kim, S. (2018). Competitive Biological Activities of Chitosan and Its Derivatives: Antimicrobial, Antioxidant, Anticancer, and Anti-Inflammatory Activities. *International Journal of Polymer Science*, 2018: 1-13. doi:10.1155/2018/1708172

Lan, J.; Ge, J.; Yu, J.; Shan, S.; Zhou, H.; Fan, S.; Zhang, Q.; Shi, X.; Wang, Q.; Zhang, L. and Wang, X. (2020). Structure of the SARS-CoV-2 spike receptor-binding domain bound to the ACE2 receptor. *Nature*, 581(7807): 215-220. doi:10.1038/s41586-020-2180-5

Leach, A. (2001). *Molecular Modelling: Principles and Applications (2nd Edition)*: Prentice Hall.

Mady, M. M. and Darwish, M. M. (2010). Effect of chitosan coating on the characteristics of DPPC liposomes. *Journal of Advanced Research*, 1(3): 187-191.

Mady, M. M.; Darwish, M. M.; Khalil, S. and Khalil, W. M. (2009). Biophysical studies on chitosan-coated liposomes. *Eur Biophys J*, 38(8): 1127-1133. doi:10.1007/s00249-009-0524-z

Mahmud, S.; Elfiky, A. A.; Amin, A.; Mohanto, S. C.; Rahman, E.; Acharjee, U. K. and Saleh, A. (2021). Targeting SARS-CoV-2 nonstructural protein 15 endoribonuclease: an in silico perspective. *Future Virol*, 16(7): 467-474 doi:10.2217/fvl-2020-0233

Morris, G. M.; Huey, R.; Lindstrom, W.; Sanner, M. F.; Belew, R. K.; Goodsell, D. S. and Olson, A. J. (2009). AutoDock4 and AutoDockTools4: Automated docking with selective receptor flexibility. *J Comput Chem*, 30(16): 2785-2791. doi:10.1002/jcc.21256

Pettersen, E. F.; Goddard, T. D.; Huang, C. C.; Couch, G. S.; Greenblatt, D. M.; Meng, E. C. and Ferrin, T. E. (2004). UCSF Chimera—a visualization system for exploratory research and analysis. *Journal of Computational Chemistry*, 25(13): 1605-1612.

Phillips, J. C.; Braun, R.; Wang, W.; Gumbart, J.; Tajkhorshid, E.; Villa, E.; Chipot, C.; Skeel, R. D.; Kalé, L. and Schulten, K. (2005). Scalable molecular dynamics with NAMD. *J Comput Chem*, 26(16): 1781-1802. doi:10.1002/jcc.20289

Saghazadeh, A. and Rezaei, N. (2020). Towards treatment planning of COVID-19: Rationale and hypothesis for the use of multiple immunosuppressive agents: Anti-antibodies, immunoglobulins, and corticosteroids. *Int Immunopharmacol*, 84: 106560. doi:10.1016/j.intimp.2020.106560

Salentin, S.; Schreiber, S.; Haupt, V. J.; Adasme, M. F. and Schroeder, M. (2015). PLIP: fully automated protein–ligand interaction profiler. *Nucleic Acids Research*, 43(W1): W443-W447.

Sonousi, A.; Mahran, H. A.; Ibrahim, I. M.; Ibrahim, M. N.; Elfiky, A. A. and Elshemey, W. M. (2021). Novel adenosine derivatives against SARS-CoV-2 RNA-dependent RNA polymerase: an *in silico* perspective. *Pharmacol Rep*, 73(6): 1754-1764. doi:10.1007/s43440-021-00300-9

South, A. M.; Diz, D. I. and Chappell, M. C. (2020). COVID-19, ACE2, and the cardiovascular consequences. *Am J Physiol Heart Circ Physiol*, 318(5): H1084-H1090. doi:10.1152/ajpheart.00217.2020

Trott, O. and Olson, A. J. (2010). AutoDock Vina: improving the speed and accuracy of docking with a new scoring function, efficient optimization, and multithreading. *J Comput Chem*, 31(2): 455-461. doi:10.1002/jcc.21334

Wilson, B.; Samanta, M. K.; Muthu, M. S. and Vinothapooshan, G. (2011). Design and evaluation of chitosan nanoparticles as novel drug carrier for the delivery of rivastigmine to treat Alzheimer's disease. *Ther Deliv*, 2(5): 599-609. doi:10.4155/tde.11.21

Wrapp, D.; Wang, N.; Corbett, K. S.; Goldsmith, J. A.; Hsieh, C.-L.; Abiona, O.; Graham, B. S. and McLellan, J. S. (2020). Cryo-EM structure of the 2019-nCoV spike in the prefusion conformation. *Science*, 367(6483): 1260-1263. doi:10.1126/science.abb2507

Zhang, J.; Xia, W.; Liu, P.; Cheng, Q.; Tahirou, T.; Gu, W. and Li, B. (2010). Chitosan modification and pharmaceutical/biomedical applications. *Marine drugs*, 8(7): 1962-1987. doi:10.3390/md8071962